

# Survey of Methods Used to Develop the Hydrogeological Model of Latvia

Aivars Spalvins<sup>1</sup>, Janis Slangens<sup>2</sup>, Inta Lace<sup>3</sup>, Kaspars Krauklis<sup>4</sup>, Olgerts Aleksans<sup>5</sup>,  
<sup>1-5</sup>Riga Technical University, Environment Modelling Centre

**Abstract** – In 2010–2012, the hydrogeological model (HM) of Latvia LAMO was established by scientists of Riga Technical University (RTU). The commercial program Groundwater Vistas (GV) is used for running LAMO. Efficient methods have been used for creating geometry of HM, the arrangement of various boundary conditions (digital terrain map, hydrographical network, infiltration flow, conditions on the HM shell surface) and for calibrating HM. Their application has considerably improved the quality of HM and reduced time needed to create LAMO.

**Keywords** – Boundary conditions, finite difference approximation, regional hydrogeological model.

## I. INTRODUCTION

This publication is focused on survey of methods [1], [2], [3] used to create LAMO. LAMO simulates the steady-state average hydrogeological situation of Latvia. LAMO covers the area of 475km–300km (Fig. 1). For the current LAMO version, the land territory of Latvia and the area of the Gulf of Riga constitute the HM active area (Fig. 2). The passive area represents border territories of the neighbouring countries. The active and passive areas are separated by the wide border zone of 4km, where boundary conditions for the active area are fixed. LAMO is open for transboundary modelling projects. The neighbouring country must provide data for activating the passive HM area involved. The vertical schematisation of LAMO is shown in Fig. 3, where geological layers are represented of the drinkable groundwater zone of Latvia. The planes 1 (rel) and 27 (D2pr) are used as places for fixing piezometric boundary conditions. The plane 2 (aer) serves as a formal aquitard that controls the computed infiltration flow. The Quaternary system and the primary Devonian layers are represented, respectively, by the planes 3-6 and 7-27. No separate layers account for the Jura and Triass systems. They are incorporated into layers 5 and 6, respectively.

To describe methods used for establishing LAMO, the basic mathematics of 3D steady-state models must be considered. By applying finite difference approximation, the  $xyz$ -grid of HM is built using ( $h \times h \times m$ ) sized blocks ( $h$  is the block plane size,  $m$  is the variable thickness of a geological layer). The model constitutes a  $p$ -tiered  $xy$ -layer system. For LAMO,  $p=27$ ,  $h=500$  metres. The 3D body of LAMO is approximated by the  $xyz$ -grid of the size  $951 \times 601 \times 27$ .

The modelling program controls the whole area of HM that contains also the passive area that takes no part in simulation. The active HM volume is enveloped by the border zone. Its outer vertical surface represents an impermeable shell that blocks a transboundary groundwater flow. Due to this fact, the



Fig. 1. Location of LAMO.

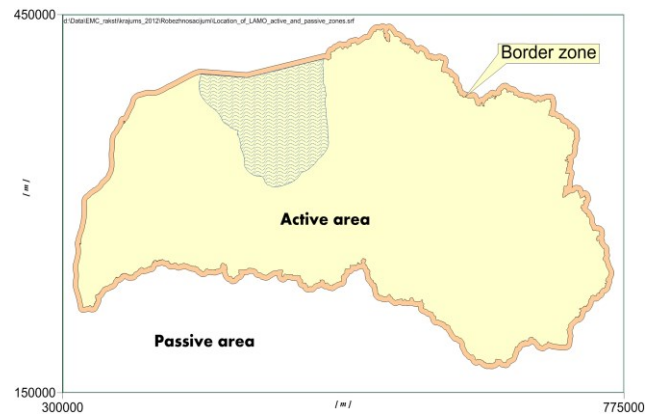


Fig. 2. Location of LAMO active and passive areas.

groundwater regime there gets distorted and axillary boundary conditions must be used to restore the normal regime.

Vector  $\varphi$  of the piezometric head is the numerical solution of the boundary field problem, which is approximated in nodes of the HM  $xyz$ -grid by the following algebraic expression:

$$A\varphi = \beta - G\psi, \quad A = A_{xy} + A_z \quad (1)$$

where  $A$  is the symmetric sparse matrix of the geological environment, which is presented by the  $xy$ -layer system containing horizontal ( $A_{xy}$  – transmissivity) and vertical ( $A_z$  – vertical hydraulic conductivity) elements of the HM grid;  $\psi$  – the boundary head vector:  $\psi_{rel}$ ,  $\psi_{bot}$ ,  $\psi_{out}$ ,  $\psi_{riv}$  – subvectors of  $\psi$  that represent boundary conditions of the HM top, bottom, border zone and rivers, respectively;  $G$  – the

diagonal matrix (part of  $A$ ) assembled by elements, linking the nodes, where  $\varphi$  must be found with the points, where  $\psi$  is given (for  $\psi_{top}$ ,  $\psi_{bot}$ ,  $\psi_{out}$  these points are nodes of the HM grid);  $\beta$  – the boundary flow vector.

The elements  $a_{xy}$ ,  $a_z$  of  $A_{xy}$ ,  $A_z$  (or  $g_{xy}$ ,  $g_z$  of  $G$ ) are computed as follows:

$$a_{xy} = k m, \quad a_z = (h^2 k)/m, \quad m_i = z_{i-1} - z_i, \quad i=1, 2, \dots, p \quad (2)$$

where  $z_{i-1}$ ,  $z_i$  are elevations, respectively, of the top and bottom surfaces of the  $i$ -th geological layer;  $z_0$  represents the ground surface elevation  $\psi_{rel}$ -map with the hydrographical network included;  $k$ ,  $m$  are, respectively, elements of digital  $m$ ,  $k$ -maps of the computed layer thickness and permeability.

If in some areas  $m_i=0$ , then the  $i$ -th layer is discontinuous. To prevent the “division by zero”, in (2),  $m_i=0$  must be replaced by small  $\varepsilon > 0$  (for LAMO,  $\varepsilon=0.02$  metres).

The set of  $z$ -maps represents the geometry of LAMO. The creating of these maps is the most burdensome task, because geometry of the geological environment of Latvia is very complex [4]. For the GV system [5], only  $z$ -maps serve as the initial ones and  $m$ -maps (thicknesses of layers) are obtained by GV itself. Appliance of  $z$ -maps is preferable, because it results in more accurate geometry of HM.

In LAMO, the  $\beta$ -vector of flows is represented only by the withdrawal rates  $\beta_w$  of wells. It is not applied to the simulation of flows on the HM top and on other boundary surfaces.

The  $\psi$ -conditions were applied, instead of the  $\beta$ -flows, due to the two main reasons:

- the  $\psi$ -conditions shortened the time needed for solving of (1), because they increased impact of the matrix  $G$  as the diagonal dominance factor of  $A$  [6, 7];
- numerical values of the  $\psi$ -conditions were known much better than the ones of the  $\beta$ -flows.

Boundary conditions  $\psi_{rel}$ ,  $\psi_{out}$ ,  $\psi_{riv}$  are the most important ones. Their arrangement is commented in Section III.

## II. INTERPOLATION OF DATA

For the  $z$ ,  $k$ -maps, interpolation surfaces represent geometrical images. Initially, for creating these maps, the RTU team used popular interpolation methods: Criging, Minimal Curvature, and Inverse Distance. Unfortunately, these methods sometimes provided erroneous results [17]. For example, if an  $m$  distribution was highly irregular, negative thicknesses appeared, even if the input data were always positive. This failure occurred, because:

- interpolated results did not hold the principle that output should remain within the minima and maxima of the input data;
- the interpolation surface did not carry “minimal energy”;
- initial data were often ignored by algorithms applied for smoothing of the interpolation result.

As conventional methods did not provide controllable interpolation results, the GDI program was developed [8], [13], [17], [18]. It gives the interpolation surface  $\sigma$ , as the numerical solution of the following associated 2D boundary problem,

| No of HM plane |  | Name of layer                   | Geological code                | HM plane code |
|----------------|--|---------------------------------|--------------------------------|---------------|
| 1.             |  | Relief                          | relh                           | relh          |
| 2.             |    | Aeration zone                   | aer                            | aer           |
| 3.             |  | Unconfined Quaternary           | Q4-3                           | Q2            |
| 4.             |    | Upper moraine                   | gQ3                            | gQ2z          |
| 5.             |  | Confined Quaternary or Jura     | Q1-3<br>J                      | Q1#           |
| 6.             |    | Lower moraine or Triass         | gQ1-3<br>T                     | gQ1#z         |
| 7.             |  | Perma Karbons Skerveles Ketleru | P2<br>C1<br>D3šk<br>D3ktl      | D3ktl#        |
| 8.             |    | Ketleru                         | D3ktl                          | D3ktlz        |
| 9.             |  | Zagares Svetes Tervetes Muru    | D3žg<br>D3sv<br>D3tr<br>D3mr   | D3zg#         |
| 10.            |    | Akmenes                         | D3ak                           | D3akz         |
| 11.            |  | Akmenes Kursas Jonisku          | D3ak<br>D3krs<br>D3jn          | D3krs#        |
| 12.            |  | Elejas Amulas                   | D3el<br>D3aml                  | D3el#z        |
| 13.            |  | Stipinu Katlesu Ogres Daugavas  | D3stp<br>D3ktl<br>D3og<br>D3dg | D3dg#         |
| 14.            |  | Daugavas Salaspils              | D3dg<br>D3slp                  | D3slp#z       |
| 15.            |  | Plavinu                         | D3pl                           | D3pl          |
| 16.            |  | Plavinu Amatas                  | D3pl<br>D3am                   | D3am#z        |
| 17.            |  | Amatas                          | D3am                           | D3am          |
| 18.            |  | Upper Gauja                     | D3gj2                          | D3gj2z        |
| 19.            |  | Upper Gauja                     | D3gj2                          | D3gj2         |
| 20.            |  | Lower Gauja                     | D3gj1                          | D3gj1z        |
| 21.            |  | Lower Gauja                     | D3gj1                          | D3gj1         |
| 22.            |  | Burtnieku                       | D2brt                          | D2brtz        |
| 23.            |  | Burtnieku                       | D2brt                          | D2brt         |
| 24.            |  | Arikula                         | D2ar                           | D2arz         |
| 25.            |  | Arikula                         | D2ar                           | D2ar          |
| 26.            |  | Narvas Narvas                   | D2nr2<br>D2nr1                 | D2nr#z        |
| 27.            |  | Pernavas                        | D2prn                          | D2pr          |

 - aquitard

# - united aquifer; #z - united aquitard

Fig. 3. Vertical schematization of LAMO.

solution of the following associated 2D boundary problem, on the  $xy$ -grid in system (1):

$$\operatorname{div}(\lambda \operatorname{grad} \sigma) = 0, \quad (3)$$

$$V \sigma = -G_{\sigma} \sigma_{\psi}, \quad V = V_{xy} - G_{\sigma} \quad (4)$$

where (4) is the algebraic equation system applied to approximate the problem (3); the matrices  $V_{xy}$ ,  $G_{\sigma}$  represent, respectively, the horizontal links  $v_{xy}$  of the interpolation grid and the elements  $g_{\sigma}$  connecting nodes, where  $\sigma$  must be found with the ones, where  $\sigma_{\psi}$  are known as initial data  $\sigma_{in}$  for the interpolation. The parameter  $\lambda(x,y)$  is used for controlling the shape of  $\sigma(x,y)$ . In areas where  $\lambda=1$ , point values  $\sigma_{in}$  usually produce sharp maxima. If  $\lambda \gg 1$  then the maxima becomes flat. Due to the changeable  $\lambda(x,y)$ , it is possible to modify the "strength" for each initial data source  $\sigma_{\psi}$ .

Fortunately for interpolation,  $\sigma$  always meets the maximum / minimum and minimal energy principles, as the fundamental feature of any solution of (3).

The GDI program mostly applies various line data as the initial ones, because they are much more informative than the pointwise data, on which the lines are based. For example, information carried by the long line profile of a river is far richer than the measured water levels of the river applied for obtaining the profile.

In GDI, any line can also be used as an impervious border, if necessary (masking of polygons, etc.).

An original program CRP has been developed for preparing the line data (isolines, geological borderlines, data of hydrographical network) and converting them into the initial data  $\sigma_{\psi}$  of the GDI program [19].

The GDI program is mainly applied to the sequential mode. During the current interpolation step, new information is used, but the results of the previous step serve as the base. In this way, a much simpler set of initial data can be applied than if one tries to obtain the final result at once. To create very complex maps, even small sets of initial root data are sufficient.

Unlike most of interpolation methods, the surface created by GDI may include sharp edges that very often are part of  $z$ -maps (tectonic faults, etc.).

### III. ARRANGEMENT OF BOUNDARY CONDITIONS

#### A. The Digital Relief Map and the head Distribution of the D2pr Aquifer

Application of the piezometric boundary condition  $\psi_{rel}$  to the HM top, instead of the conventional  $\beta_{inf}$ -conditions for infiltration, has considerably reduced the effort of developing large regional models, where the infiltration distribution is very complex. It must account for numerous recharge and discharge areas. If HM contains many geological layers then it is virtually impossible to predict the response of HM to a fixed  $\beta_{inf}$  and the computed value of  $\varphi$  often occurs above the ground surface  $\psi_{rel}$ .

The  $\psi_{rel}$ -map was obtained by using the data of the Geospatial Information Agency of Latvia. Methods used to

create the map are described in [9]. The GDI program was applied to account both for ground surface elevation isolines and parameters of the hydrographical network.

If the  $\psi_{rel}$  - map is used, the flow  $q_{inf}=q_{aer}$  passes through the aeration zone:

$$q_{aer} = G_{aer}(\psi_{rel} - \varphi_{Q2}) \quad (5)$$

where  $\varphi_{Q2}$  is the computed head (subvector of  $\varphi$ ) for the aquifer  $Q2$ ;  $G_{aer}$  (diagonal submatrix of  $G$ ) contains the vertical links  $g_{aer}$  of the aeration zone connecting the fixed  $\psi_{rel}$  with the computed  $\varphi_{Q2}$ . The expression (5) gives the ordinary result of HM, when  $\psi$ -conditions are applied. As a rule, even the first run of HM provides the following feasible results:

- the surface  $\varphi_{Q2}$  automatically follows main geometrical features of  $\psi_{rel}$ , because  $g_{aer}$  interlinks both surfaces; in humid areas this natural phenomenon always occurs;
- it follows from (5) that components of  $q_{aer}$  respond correctly ( $q_{aer}$  increases) to a decrease of  $\varphi_{Q2}$  caused by the flow of wells  $\beta_w$ ; when fixed  $\beta_{inf}$  is used, this natural response is not automatically accounted for;
- HM provides the  $q_{aer}$  distribution, which defines variable infiltration intensity and clearly indicates the areas of discharge and recharge.

The advantage of  $q_{aer}$  obtained by HM itself over a conventional fixed  $\beta_{inf}$  distribution is considerable, because  $q_{aer}$  is based on much more reliable initial data than any fixed  $\beta_{inf}$  distribution. The data are carried mostly by  $\psi_{rel}$  and the system (1), as a whole.

The vertical links  $g_{aer}$  of the diagonal matrix  $G_{aer}$  are controlling the  $q_{aer}$  distribution. Values  $g_{aer}$  depend on  $h^2$ ,  $k_{aer}$  and  $m_{aer}$  (formula (2));  $k_{aer}$  and  $m_{aer}$  are, respectively, the permeability and the thickness of the aeration zone. Initially,  $k_{aer}$  and  $m_{aer}$  are unknown. In nature,  $m_{aer} = \psi_{rel} - \varphi_{Q2}$  if  $q_{aer} > 0$ . If  $q_{aer} < 0$  then, in LAMO,  $m_{aer} = 0.02$ . The negative infiltration flow is caused mainly by lowlands, rivers and lakes. First, the following values of the aeration zone were tried:  $m_{aer} = 0.02$  [m],  $k_{aer} = 10^{-6}$  [m/day] (for recharge areas);  $k_{aer} = 10^{-4}$  [m/day] (for areas of lakes and sea);  $k_{aer} = 10^{-8}$  [m/day] (for areas of swamps).

To avoid iterative changes of the HM geometry, during calibration of HM,  $m_{aer} = 0.02$  was kept constant, until the calibrated  $q_{aer}$ -flow was obtained (Fig. 7) by adjusting the  $k_{aer}$ -distribution. This uncommon assumption is permissible. It was explained in [1], [20] that in order to avoid any change of the geometry, the real thicknesses of layers (in our case,  $m_{aer}$  and  $m_{Q2}$ ) may not be applied during calibration.

The piezometric head distribution  $\psi_{D2pr}$  of the D2pr aquifer is applied as the boundary condition to the LAMO bottom plane ( $p=27$ ). The  $\psi_{D2pr}$ -map was obtained by using information of [16]. Influence of  $\psi_{D2pr}$  is small, because it is separated from the HM body by the thick regional D2nr aquitard (see Fig. 4).

There are two reasons for application of this boundary condition: it may be useful if a modeller carries out research regarding the role of tectonic faults of the D2nr aquitard; the D2pr aquifer contains drinking water in the northeast part of Latvia.

### B. Design of Boundary Conditions for the Border Zone

Due to the presence of the HM passive area, the outer vertical surface of the boundary zone (shell) is impermeable for the transboundary groundwater flow. This causes distortion of the natural groundwater regime at the vicinity of the shell. One must try to recover the regime on the inner surface of the border zone. It can be done by fixing auxiliary boundary conditions  $\psi_{out}$  on the middle line of the zone. As the initial data for obtaining  $\psi_{out}$  of aquifers, three data sources were used that provided linewise information (as slices along the zone middle line): the  $\psi_{rel}$ -map; the D2ar aquifer map of  $\varphi_{D2ar}$ ; the map  $\varphi_{preQ}$  of the prequaternary surface. The distribution  $\varphi_{preQ}$  was prepared by the Latvian Environment, Geology and Meteorology Centre (LEGMC). The  $\varphi_{preQ}$ -surface can provide only fragments of  $\psi_{out}$  that can be observed from the bird's eye view. Special software was developed for extracting these data and for providing information that was necessary to design the interpolation tool that provided  $\psi_{out}$  for other aquifers. The design is based on the fact that there is a set of vertical links  $a_z$  that joins the neighbouring aquifers along the middle line of the border zone. These links account both for the  $k$  and  $m$  parameters of aquitards (2). If values of these links are considerably enlarged (at least, 1000 times), then this set of the transformed links behaves like a spatial interpolator.

Therefore, the boundary condition  $\psi_{out}$  is supported by HM itself, as follows: on the middle line of the border zone, the components  $\psi_{out}$  originated from the  $\psi_{rel}$ ,  $\varphi_{D2ar}$ ,  $\varphi_{preQ}$ -maps are fixed as the initial ones; the other components of  $\psi_{out}$  are provided by the set of transformed  $a_z$ -links. The interpolator is not a part of the LAMO active volume and it can be used permanently. This feature is very useful during the HM calibration when  $k$ -maps are changed and the conditions  $\psi_{out}$  follow these adjustments.

### C. Rivers as Boundary Conditions

The condition  $\psi_{riv}$  that represents water levels of rivers is attached to inner nodes of the HM grid via the elements of the river bed conductance matrix  $G_{riv}$ . The flow  $q_{riv}$  caused by rivers is given by the expression:

$$q_{riv} = G_{riv} (\varphi_{riv} - \psi_{riv}) \quad (6)$$

where the diagonal matrix  $G_{riv}$  is part of  $G$ ;  $\psi_{riv}$  is the subvector of  $\psi$ ,  $\varphi_{riv}$  represents these nodes, where the corresponding components of  $\psi_{riv}$  that represent long line profiles of rivers are attached via the links belonging to  $G_{riv}$ . Components of  $\psi_{riv}$  are fixed in nodes located outside the HM grid. The value of a single element  $g_{riv}$  of  $G_{riv}$  is presented by the formula:

$$g_{riv} = h w_{riv} k_{riv} / m_{riv} \quad (7)$$

where  $h=500$  (plane step);  $w_{riv}$  – the river width;  $k_{riv}$ ,  $m_{riv}$  – permeability and thickness of the river bed layer, respectively; these two parameters are unknown. Value  $m_{riv}=1$  was fixed and  $k_{riv}=0.02$  was found experimentally. Therefore, as the initial try, the formula (7) gives  $g_{riv}=10w_{riv}$ . For LAMO, rivers are presented by their middle lines. An exception is of

the Daugava River. It includes three artificial lakes of hydroelectric power plants of Riga, Kegums, Plavinas.

To obtain the  $\psi_{riv}$ -conditions (formulas (6) and (7)), the following items must be prepared: the  $xy$ -location of a river line; the long line profile (water levels  $\psi_{riv}$  of a river); the width  $w_{riv}$  of a river; the  $z$ -attachment of a river that accounts for the fact that a river, on its run, may be joined with different geological layers. For example, the Gauja River runs through the Quaternary, the upper and lower Devonian layers. It was necessary to develop special software to prepare data for the  $\psi_{riv}$ -conditions.

At present, the empirical values  $k_{riv}=0.02$ ,  $m_{riv}=1$  are applied to all rivers. In nature,  $k_{riv}$  may be different not only for each river, but also for their fragments. The elements  $g_{riv}$  can be controlled also by changing the value of  $m_{riv}$ . The task of finding more realistic  $g_{riv}$  distributions is very complex, because river flows of (6) measured in nature must be used. Knowledge of these flows will provide more exact estimates of the interaction between groundwater and rivers. The task of making use of this information is part of the LAMO future development.

## IV. CREATION OF Z-MAPS

The most time-consuming part of developing LAMO was the preparation of digital  $z$ -maps that served as initial data for the GV system. For LAMO, most layers are outcropping (Fig. 4). They are not continuous, and for this reason, they do not exist everywhere.

The geometry of LAMO is based on the geological information accumulated by LEGMC. The information includes stratigraphical data of boreholes, geological maps and descriptions regarding geology of Latvia.

The LAMO geometry results in the set of  $z$ -maps. It includes 28 surfaces for 27 geological layers presented in HM (see Fig. 3). The top surface of HM ( $z=0$ ) is the digital hydrogeological relief of Latvia. It includes the hydrographical network (rivers, lakes, sea). The  $z=1$  surface is the digital geological relief. It represents the ground surface elevations. For LAMO, this map accounts for depth of the sea and of three artificial lakes of hydroelectric power plants of the Daugava River.

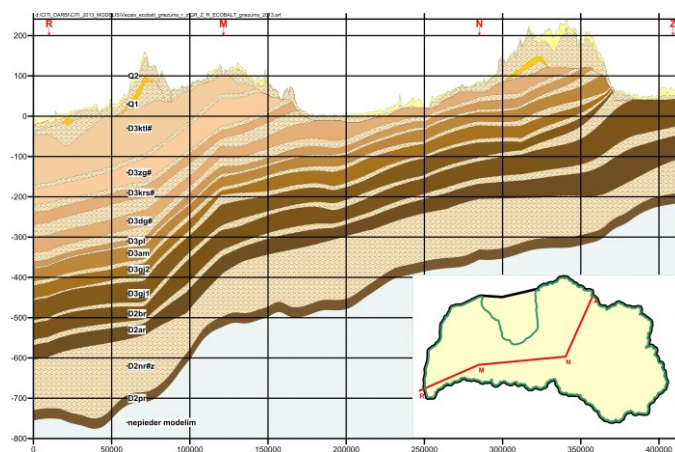


Fig. 4. Geological cross section.

The LEGMC specialists have prepared two important geological maps: the prequaternary surface preQ ( $z=6$ ), the D2pr surface ( $z=26$ ). They are presented in Fig. 5 and Fig. 6, respectively. The volumes of the Quaternary and primary geological layers are included between  $z=0$ ,  $z=6$  and  $z=6$ ,  $z=27$  surfaces, respectively.

The most time-consuming and difficult task [10] was the creation of  $z$ -maps for the primary geological layers ( $z=7, 8, \dots, 27$ ). The basic stratigraphical information was carried by the boreholes and elevations of geological borderlines located on the preQ surface (Fig. 5). However, very often data of boreholes were contradictory and it was not always possible to amend them. To reduce laborious work of checking the quality of all available borehole data, the set of representing geological cross sections was used, where the chosen boreholes with trustworthy data were located. Deep boreholes were used, which provided stratigraphical data for all geological layers of HM. As a rule, data gaps occurred along a section laterally and vertically (along a borehole axis). These gaps were filled by complementary data that were concordant with the existing borehole data. The  $z$ -maps must always give positive thicknesses  $m$ . For this reason, the data of the sections must match this condition for layers of HM.

The  $m=0$  areas of discontinuous layers also must be accounted for. It is done by using  $m=\varepsilon=0.02$  instead of the zero thickness. There are three main reasons why  $\varepsilon$  must be small: geometrical distortions are minimal even if the number of overlaying  $m=0$  areas is large (the northern part of Latvia); transmissivity  $T=\varepsilon k$  of aquifers is small even if their  $k$  is large; conductivity  $g_v$  of aquitards  $g_v=h^2k/\varepsilon$  is great even if their  $k$  is very small.

If  $\varepsilon=0.02$  then LAMO in its  $m=0$  areas behave normally without special control measures for outcropping strata. This first stage of preparing  $z$ -maps was performed by using the EXCEL system [12].

During the second stage, the SURFER system [11] was applied to obtain a preliminary version of  $z$ -maps. The pointwise data prepared by EXCEL and data of the geological borderlines were used by SURFER.

Unfortunately, SURFER cannot provide good  $z$ -maps, because of the following reasons: only pointwise data can be processed and their number is limited; the maximum – minimum principle is not insured for output data; the condition  $m>0$  is often violated; for the  $m=0$  areas, the requirement  $\varepsilon=0.02$  is neglected. However, results obtained by SURFER provided valuable information for correcting possible errors of initial data.

The final version of  $z$ -maps was obtained by the GDI system. It applied data of the representing cross sections, of the geological borderlines and of surfaces that were extracted from the preQ surface map (Fig. 5).

Geometry of buried valleys in the body of primary geological layers was not simulated by LAMO. Accounting for the buried valleys is difficult and the data about the material that fills them are uncertain.

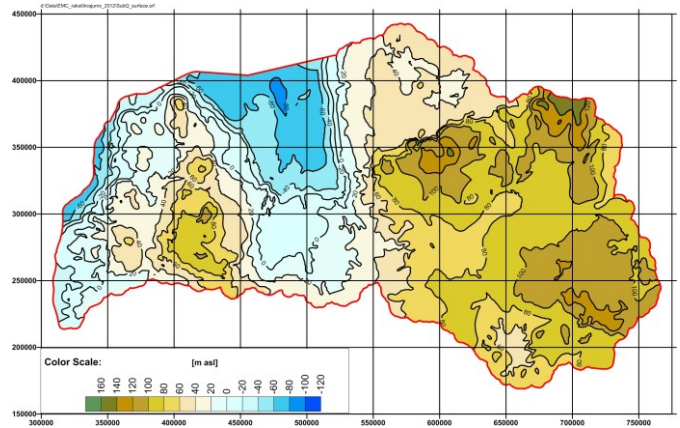


Fig. 5. The prequaternary preQ surface ( $z=6$ ).

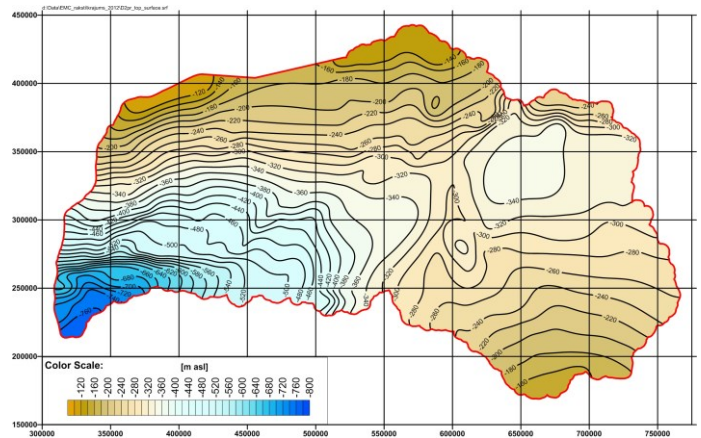


Fig. 6. The D2pr top surface ( $z=26$ ).

## V. CALIBRATION PROCESS

After all the necessary digital maps are uploaded into the GV system, the model starts functioning and its calibration has to be accomplished.

Due to unavoidable limitations in the initial data, HM has no unique solution of (1). Calibration of HM is a controlled iterative process, involving the addition of complementary data, until HM of a required quality is obtained. The quality is checked and maintained by tracing calibration targets. The following targets are usually set:

- original data should not be contradicted by data generated by HM; for example, the  $\psi$  and  $\varphi$  distributions of (1) must reproduce observed head values, matrix  $A$  must incorporate the observed permeability and geometrical features of  $k$  and  $z$ -maps, etc.;
- within the HM body, groundwater flows should not reach unnatural values (infiltration flow, flows regarding the hydrological network, etc.);
- results of HM must confirm the real hydrogeological situation, because a formal agreement between the computed and observed target data does not assure correct simulation.

The calibration will never succeed if serious errors of data are present. Problems can include faults in data coordinates or values, mistakes in the geological layer identification, mismatched reference data, unreliable boundary conditions or inadequate software.

The main subjects controlled during LAMO calibration were k-maps of aquitards, because their distributions of  $k$  were unknown.

A valuable instrument of searching for the right k-maps was the data of vertical flows between neighbouring layers.

The flows were computed by SURFER as follows:

$$q_{i,i+1} = 0.73 \times 10^6 (\varphi_i - \varphi_{i+1}) / (m_i / k_i + m_{i+1} / k_{i+1}) \quad (8)$$

where  $q_{i,i+1}$  was the vertical flow [mm/year] passing between the  $i$ -th and  $i+1$ -th layers. The formula holds even if both thicknesses  $m_i$  and  $m_{i+1}$  are representing  $\varepsilon=0.02$  areas.

The k-maps have the following structure:

$$k = k_c k_{out} \quad (9)$$

where  $k_c$  and  $k_{out}$  are, respectively, the core and outer diagonal k-matrixes. The  $k_c$  matrix has no dimension and its basic value is 1.0. In the course of calibration, some  $k_c$  must be changed to values that are larger or smaller than the base value 1. The

matrix  $k_{out}$  serves as the general factor for controlling the k-map for all nodes of an HM grid plane. The GDI program was used to obtain  $k_c$ -maps. The calibration of the  $k_{aer}$ -map for the aeration zone (aer) is important. Initially, its core matrix  $k_c$  values are 100.0 and 0.01 for areas of lakes and swamp areas, respectively. The following formula was used for correcting the initial  $k_c$  matrix:

$$k_c = k_c c, \quad c=1, \text{ if } \Delta \leq M \quad \text{or} \quad c=(M/\Delta)^n \\ \text{if } \Delta > M, \quad \Delta = \psi_{rel} - \varphi_{Q2} \quad (10)$$

where  $c$  is the correction matrix; the parameter  $M$  accounts for limitedness of the flow if  $\Delta > M$  [metres].

For the areas, where  $\Delta > M$ , the flow  $q_{aer}$  gets limited as follows:

$$q_{aer} = k_{aer} M^n \Delta^{1-n} / 0.02. \quad (11)$$

If  $n=1$ ,  $q_{aer}$  does not depend on  $\Delta$ . Then  $q_{aer}$  is controlled by the parameters  $k_{aer}$  and  $M$ . For LAMO, the empirical values  $M=4$  and  $n=0.75$  were used.

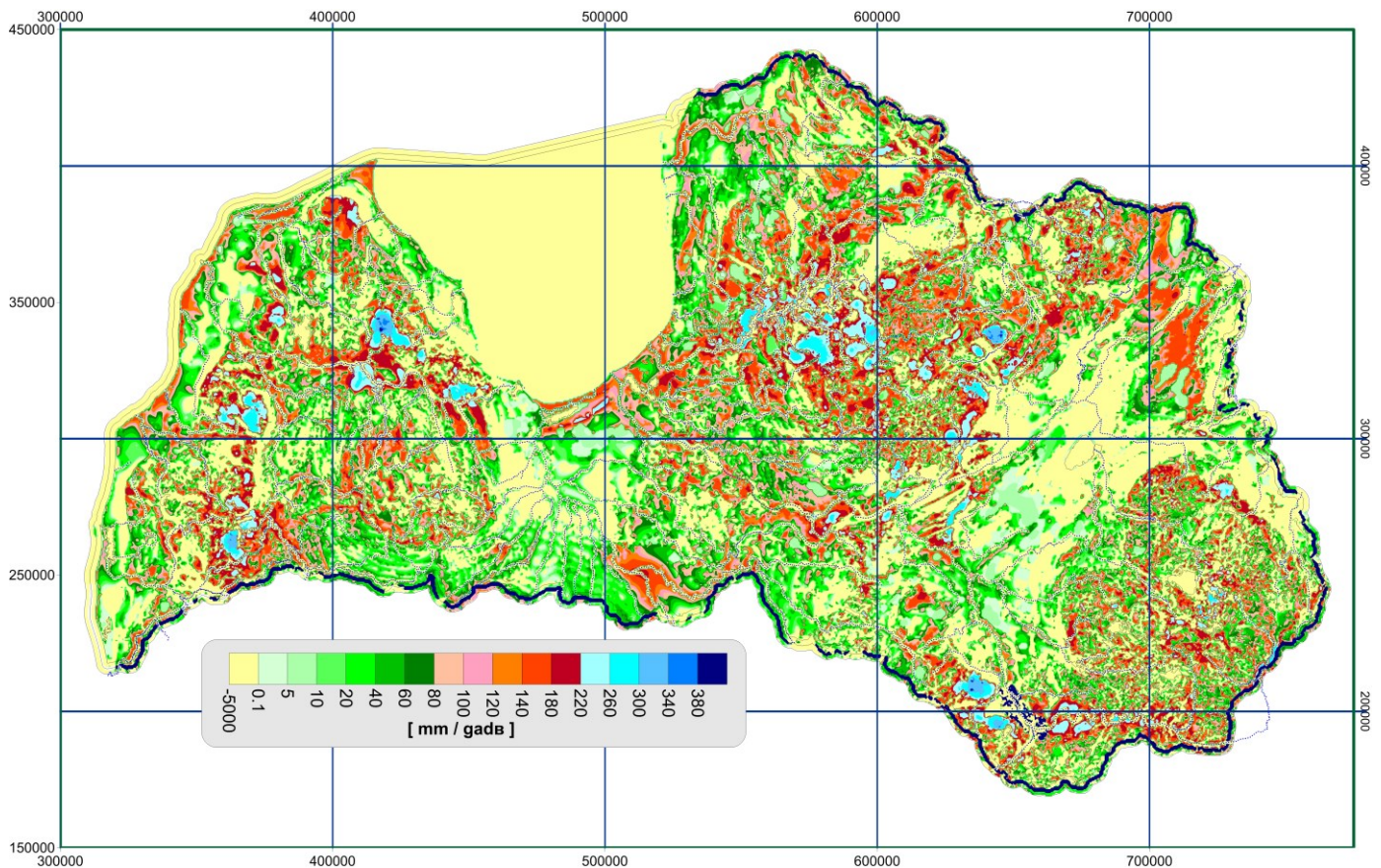


Fig. 7. Calibrated  $q_{aer}$  distribution [mm/year].

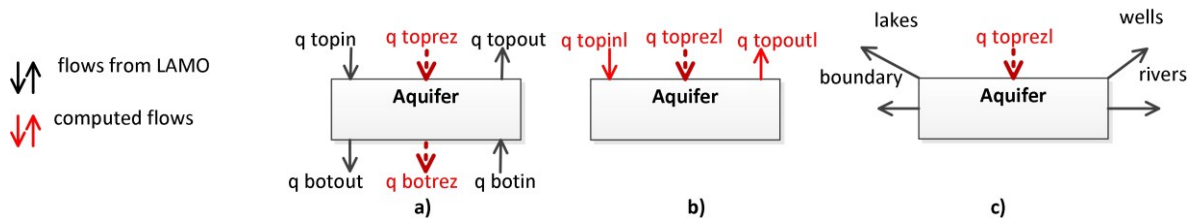


Fig. 8. Legend of stages a), b), c) for obtaining flows of Table I:

- a) computing of resulting flows:  $q_{toprez}$ ,  $q_{botrez}$ ;  
 b) computing of local flows  $q_{topinl}$ ,  $q_{topoutl}$ ,  $q_{toprezl}$ ;  
 c) local balance of aquifer.

TABLE I  
 GROUNDWATER FLOWS OF AQUIFERS, THOUS.M<sup>3</sup>/DAY (PRELIMINARY VERSION)

| Name of aquifer | $q_{topin}$ | $q_{topout}$ | $q_{toprez}$<br>(2+3) | $q_{botout}$ | $q_{botin}$ | $q_{botrez}$<br>(5+6) | $q_{topinl}$<br>(2+5) | $q_{topoutl}$<br>(3+6) | $q_{toprezl}$<br>(4+7)<br>(8+9) | rivers | lakes | boundary | i wells |
|-----------------|-------------|--------------|-----------------------|--------------|-------------|-----------------------|-----------------------|------------------------|---------------------------------|--------|-------|----------|---------|
| 1               | 2           | 3            | 4                     | 5            | 6           | 7                     | 8                     | 9                      | 10                              | 11     | 12    | 13       | 14      |
| Q2              | 11194       | -3775        | 7419                  | -6992        | 3461        | -3531                 | 4202                  | -314                   | 3888                            | -3288  | -426  | -118     | -56     |
| Q1#             | 6992        | -3461        | 3531                  | -6855        | 3349        | -3506                 | 137                   | -112                   | 25                              | -7     | 0     | -18      | 0       |
| D3ktl#          | 6855        | -3349        | 3506                  | -6524        | 3191        | -3333                 | 331                   | -158                   | 173                             | -192   | 0     | 20       | -1      |
| D3zg#           | 6524        | -3191        | 3333                  | -6284        | 3014        | -3270                 | 240                   | -177                   | 63                              | -41    | 0     | -18      | -4      |
| D3krs           | 6284        | -3014        | 3270                  | -6333        | 2986        | -3247                 | 51                    | -28                    | 23                              | -11    | 0     | -8       | -4      |
| D3dg#           | 6233        | -2986        | 3247                  | -4981        | 2333        | -2648                 | 1252                  | -653                   | 599                             | -569   | -10   | -15      | -5      |
| D3pl            | 4981        | -2333        | 2648                  | -3981        | 1849        | -2132                 | 1000                  | -484                   | 516                             | -446   | 8     | -70      | -8      |
| D3am            | 3981        | -1894        | 2132                  | -3622        | 1634        | -1988                 | 359                   | -212                   | 144                             | -93    | 0     | -50      | -1      |
| D3gj2           | 3622        | -1634        | 1988                  | -3041        | 1418        | -1623                 | 581                   | -216                   | 365                             | -244   | 0     | -96      | -25     |
| D3gj1           | 3041        | -1418        | 1623                  | -2114        | 996         | -1118                 | 927                   | -412                   | 505                             | -327   | 0     | -154     | -24     |
| D2brt           | 2114        | -996         | 1118                  | -852         | 423         | -429                  | 1262                  | -573                   | 689                             | -462   | 0     | -214     | -13     |
| D2ar            | 652         | -423         | 429                   | -256         | 36          | -220                  | 596                   | -387                   | 209                             | 0      | 0     | -195     | -14     |
| Model           | 11194       | -3775        | 7419                  | -256         | 36          | -220                  | 10938                 | -3739                  | 7199                            | -5680  | -428  | -936     | -155    |
| Q1+Q2           | 11194       | -3775        | 7419                  | -6855        | 3349        | -3506                 | 4339                  | -426                   | 3913                            | -3295  | -426  | -136     | -56     |
| Primary         | 6855        | -3349        | 3506                  | -256         | 36          | -220                  | 6599                  | -3313                  | 3286                            | -2385  | -2    | -800     | -99     |

If  $n=1$ ,  $q_{aer}$  does not depend on  $\Delta$ . Then  $q_{aer}$  is controlled by the parameters  $k_{aer}$  and  $M$ . For LAMO, the empirical values  $M=4$  and  $n=0.75$  were used.

By using the rule (11), a rather smooth limitation of the infiltration flow  $q_{aer}$  was achieved for highland areas (Fig. 7). The formula (11) was used also for other aquitards of HM.

During the calibration process, the thickness  $m_{aer}=0.02$  of the aeration zone is kept unchanged. As the final step, the real thickness  $m_{aer}$  must be obtained:

$$m_{aer}=0.02 \text{ if } \Delta \leq 0.02 \text{ or } m_{aer}=\Delta \text{ if } \Delta > 0.02$$

$$\Delta = \psi_{rel} - \varphi_{Q2}, \quad k_{aer} = (k_{aer})_c c, \quad c = m_{aer} / 0.02 \quad (12)$$

where  $(k_{aer})_c$  is the calibrated value and  $c$  is the correction matrix where its elements have values 1 and  $m_{aer} / 0.02$  if  $m_{ae}=0.02$  and  $\Delta$ , respectively.

If for the zone aer, its real thickness  $m_{aer}$  is obtained then the thickness  $(m_{Q2})_c$  decreases:  $m_{Q2}=(m_{Q2})_c - m_{aer}$ .

It may occur that  $m_{Q2}<0$ . It means that the Q2 aquifer is drained. To avoid further variations of the HM geometry (change of  $m$  for gQ2z aquitard), the assumption was made that at least 0.2 metres of the Q2 aquifer remained saturated.

This assumption holds if  $m_{aer}$  is changed as follows:

$$(m_{aer})_c = m_{aer} \text{ if } m_{Q2} > 0.2 \text{ or } (m_{aer})_c = c m_{aer}$$

$$\text{if } m_{Q2} \leq 0.2, \quad c = (1 + (m_{Q2} - 0.2) / m_{aer}); \quad (13)$$

$$\text{when } c m_{aer} < 0.02 \text{ then } (m_{aer})_c = 0.02$$

where  $(m_{aer})_c$  is the changed value of  $m_{aer}$ ;  $c \leq 1$  is the correction factor.

After dewatering of some areas for the Q2 aquifer, it was necessary to continue the calibration process, because this change of the geometry was not supported by the transformation of (12).

At present, the residual (difference between monitored and computed  $\varphi$  values) does not exceed 1.7 metres (a quadratic error) and 2% (a relative error).

The preliminary version of the flow distribution for LAMO aquifers is presented in Table I. The total flow of rivers  $q_{riv}$  was the calibration target. Its rough value was obtained from the book [16].

Figure 8 gives the legend of the sequential stages a), b), c) performed to obtain Table I. The stage a) represents computing of the resulting flows  $q_{toprez}$  and  $q_{botrez}$  (columns 4 and 7), respectively, on the top and bottom surfaces of an aquifer:

$$q_{toprez}=q_{topin}+q_{topout}; \quad q_{botrez}=q_{botout}+q_{botin} \quad (14)$$

where the flows  $q_{topin}$ ,  $q_{topout}$ ,  $q_{botout}$ ,  $q_{botin}$  (columns 2, 3, 5, 6) are taken from the groundwater balance output of the GV system.

The stage b) provides local flows  $q_{topinl}$ ,  $q_{topoutl}$ ,  $q_{toprezl}$  (columns 8, 9, 10):

$$\begin{aligned} q_{topinl} &= q_{topin} + q_{botout}; & q_{topoutl} &= q_{topout} + q_{botin} \\ q_{toprezl} &= q_{topinl} + q_{topoutl} = q_{toprez} + q_{botrez} \end{aligned} \quad (15)$$

By using expressions (15), the vertical groundwater transit flows are excluded from the aquifer balance. The flows  $q_{toprezl}$ ,  $q_{river}$ ,  $q_{border}$ ,  $q_{wells}$  (columns 10, 11, 12, 13, 14) constitute local balance of the aquifer (stage c)). The flows  $q_{river}$ ,  $q_{lakes}$ ,  $q_{border}$ ,  $q_{wells}$  are given in the GV mass balance sheet.

Comparison of the local resulting flows  $q_{toprezl}$  provides clear information about the impact of each aquifer on the total balance (7199thous.m<sup>3</sup>/day) of HM. Table I also provides summary for the Quaternary (Q1+Q2) and the primary layers: 3913thous.m<sup>3</sup>/day and 3286thous.m<sup>3</sup>/day, respectively.

By using data about the total infiltration, one can compute the mean infiltration [mm/year] on the land territory of Latvia (64.5thous.km<sup>2</sup>):

$$(11194 \times 0.365)/64.5 = 63 \text{ [mm/year].}$$

This recharge of groundwater resources composes 9.0% of the mean precipitation (700mm/year) for Latvia.

However, the calibration process of LAMO is not completed, because the links of the hydrographical network with the HM body have not been properly adjusted yet.

## VI. CONCLUSIONS

The hydrogeological model of Latvia has been developed. To create the model, original methods have been used to obtain maps representing complex geometry of the geological environment of Latvia and to arrange various types of boundary conditions (digital relief map, conditions regarding hydrographical network, etc.). Effective methods have used to calibrate HM. The knowledge and ideas presented in this paper may be useful for modellers dealing with the problem of creating highly complex HM.

## ACKNOWLEDGEMENTS

The hydrogeological model of Latvia LAMO has been developed within the framework of the project "The Creating of Hydrogeological Model of Latvia to be Used for Management of Groundwater Resources and for Evaluation of Their Recovery Measures". The project has been co-financed by the European Regional Development Fund.

## REFERENCES

- [1] Spalvins, A., Slangens, J., Krauklis, K., Lace, I. Methods and tools to be applied for creating of regional hydrogeological model of Latvia. In: *25th European Conference on Modelling and Simulation*, June 7-10, 2011, Krakow, Poland, pp. 132-141, (ISBN: 978-0-9564944-2-9)
- [2] Spalvins, A., Slangens, J., Aleksans, O., Krauklis, K., Lace, I. Regional hydrogeological model of Latvia for management of its groundwater resources, In: *5-th International scientific conference Applied information and communication technologies*, 24-26 April 2012, Jelgava, Latvia, pp. 135-155 (CD) (ISBN (78-9984-48-065-7)-2).
- [3] Spalvins, A., Slangens, Lace, I., J., Krauklis, K., Skibelis, V., Aleksans, O., Levina, N. Hydrogeological model of Latvia, first results. *Scientific Journal of Riga Technical University Boundary Field Problems and Computer Simulation*. 51-th issue, Riga, RTU, 2012, pp. 4-13, ISSN 1407 – 7493
- [4] Paskevicius, J. *The geology of the Baltic republics*. Vilnius University, Vilnius, 1997, p. 387, ISBN 9986-623-20-0
- [5] Environmental Simulations, Inc. *Groundwater Vistas. Version 6*, Guide to using, 2011
- [6] Strang, G. *Linear algebra and its applications*. Academic Press, New York, 1976, p. 373 INC.
- [7] Spalvins, A., Slangens, J. Impact of boundary conditions on quality of hydrogeological models. *Proceedings of Riga Technical University in series Computer Science. Boundary Field Problems and Computer Simulation*. vol. 5, 33(49)-th issue. Riga: RTU, 2007, pp. 108-116, ISSN 1407-7493.
- [8] Spalvins, A. Modelling as a powerful tool for predicting hydrogeological change in urban and industrial areas. *K.W.F. Howard and R.G. Israfilov (eds.) Current problems of Hydrology in Urban Areas. Urban Agglomerates and Industrial Centres*. Kluwer Academic Publishers. Printed in Netherlands, 2002, pp. 57-75.
- [9] Slangens, J., Krauklis, K. Creating of digital relief map for regional hydrogeological model of Latvia. *Scientific Journal of Riga Technical University in series "Computer Science". Boundary Field Problems and Computer Simulation*. vol. 5, 49. (53)-th issue, Riga, RTU, 2011, pp. 21-25, ISSN 1407 – 7493
- [10] Spalvins, A., Slangens, J., Lace, I., Krauklis, K., Aleksans, O., Levina, N. Methods and software tools used to designate geometry for regional hydrogeological model of Latvia. *Scientific Journal of Riga Technical University. Boundary Field Problems and Computer Simulation*, 51-th issue, Riga, RTU, 2012, pp. 13-19, ISSN 2255-9124
- [11] Golden Software. *SURFER-9 for Windows*, Users Manual, 2010
- [12] Walkenbach, J. *Excel 2007 Bible*. Wiley Publishing, Inc., Indianapolis, Indiana, 2007, p. 808
- [13] Spalvins, A., Slangens, J. Reliable data interpolation method for a hydrogeological model conductivity matrix. In: *Sixth International Conference on Calibration and Reliability in Groundwater Modeling. Credibility in Modelling*. Vol.2, 9-13 September 2007, Copenhagen, Denmark, pp. 137-142
- [14] Spalvins, A., Slangens, J., Lace, I., Krauklis, K. Arrangement of boundary conditions for hydrogeological model of Latvia. *Scientific Journal of Riga Technical University. Boundary Field Problems and Computer Simulation*. 51-th issue, Riga, RTU, 2012, pp. 20-24, ISSN 2255-9124
- [15] Spalvins, A., Slangens, J., Lace, I., Krauklis, K., Skibelis, V. Creating of initial data maps for regional hydrogeological model of Latvia. *Scientific Journal of Riga Technical University in series "Computer Science". Boundary Field Problems and Computer Simulation*. vol. 5, 50-th issue. Riga: RTU, 2011, pp. 14-22, ISSN 1407 – 7493
- [16] Dzilna, I. *Resources, composition and dynamics of groundwater for the middle part of the Baltic area*. Zinatne, Riga, 1970, p. 197 (in Russian)
- [17] Spalvins, A., Slangens, J. Numerical interpolation of geological environment data. In: *Boundary Field problems and Computers, Proc. of Latvian-Danish Seminar on "Groundwater and Geothermal Energy"*. Riga-Copenhagen, 35-th issue, RTU, 1994, pp. 181-196.
- [18] Spalvins, A., Slangens, J., Krauklis, K. Updating of geological data interpolation programs. *Scientific Proceedings of Riga Technical University in series "Computer Science"*, Boundary Field Problems and Computer Simulation. 33(49)-th issue, - Riga, 2007, pp. 118-129. ISBN 1407 - 7493
- [19] Spalvins, A., Slangens, J. Reliable program for preparing line data of hydrogeological models. *Scientific Proc. of Riga technical university in series "Computer science"*, *Boundary Field Problems and Computer simulation*. vol. 4, 42 -th issue. Riga: RTU, 2000, pp. 45-53. ISSN 1407-7493.
- [20] Spalvins, A., Slangens, J., Lace, I., Stuopis, A., Domasevicius, A. Creating of Regional Hydrogeological Model for the South-East of Lithuania. In: *Proceedings of XXXVIII IAH Congress Groundwater Quality Sustainability, Extended Abstracts (CD)*. Poland, Krakow, September 12-17, 2010, pp. 1233-1238.



**Aivars Spalvins** was born in Latvia. In 1963, he graduated from Riga Polytechnical Institute (since 1990, Riga Technical University) as a Computer Engineer. In 1967, A. Spalvins received the Degree of Candidate of Sciences. (Dr.sc.ing.). A. Spalvins has been with the university since 1958 (as a student) until now. He is the Head of the Environment Modelling Centre of the University. His present scientific interests

include computer modelling of groundwater flows and migration of contaminants.  
E-mail: emc@cs.rtu.lv



**Janis Slangens** was born in Latvia. In 1969, he graduated from Riga Polytechnical Institute (since 1990, Riga Technical University) as a Computer Engineer. In 1985, J. Slangens received the Degree of Candidate of Sciences (Dr.sc.ing.). Since 1969, he has been working at the University. He is a Senior Researcher at the Environment Modelling Centre. His present scientific interests include computer modelling of groundwater flows.

E-mail: emc@cs.rtu.lv



**Inta Lace** was born in Latvia. In 1971, she graduated from Riga Polytechnical Institute (since 1990, Riga Technical University) as a Computer Engineer. In 1995, I. Lace received the Master's Degree in Applied Computer Science. Since 1991, she has been a Researcher at the Environment Modelling Centre, the Faculty of Computer Science and Information Technology.  
E-mail: emc@cs.rtu.lv



**Olgerts Aleksans** was born in Latvia. In 1979, he graduated from Vilnius State University (since 1988, the University of Vilnius) as a Hydrogeologist & Engineering Geologist. In 2011, O. Aleksans received the Doctoral Degree in Geology from the University of Latvia. In the time period from 1997 till 2011 he was one of the company's VentEko Ltd founders and its Scientific Director. Since 2011 he has been working as a

Researcher at the Environment Modeling Centre of Riga Technical University.  
E-mail: olgerts.aleksans@gmail.com



**Kaspars Krauklis** holds the Master's Degree in Computer Systems from Riga Technical University (2007) and the Certificate in Teaching of Engineering Sciences from the Institute of Humanities, RTU (2005). At present, he works as a Researcher at the Environment Modelling Centre of Riga Technical University.  
E-mail: emc@cs.rtu.lv